TISSUE ENGINEERING: Part A
Volume 16, Number 1, 2010

DOI: 10.1089/ten.tea.2009.0164

Bone Grafts Engineered from Human Adipose-Derived Stem Cells in Perfusion Bioreactor Culture

Mirjam Fröhlich, B.Sc.,[1,2] Warren L. Grayson, Ph.D.,[1] Darja Marolt, Ph.D.,[1] Jeffrey M. Gimble, M.D., Ph.D.,[3] Nevenka Kregar-Velikonja, Ph.D.,[2] and Gordana Vunjak-Novakovic, Ph.D.[1]

We report engineering of half-centimeter–sized bone constructs created *in vitro* using human adipose-derived stem cells (hASCs), decellularized bone scaffolds, and perfusion bioreactors. The hASCs are easily accessible, can be used in an autologous fashion, are rapidly expanded in culture, and are capable of osteogenic differentiation. hASCs from four donors were characterized for their osteogenic capacity, and one representative cell population was used for tissue engineering experiments. Culture-expanded hASCs were seeded on fully decellularized native bone scaffolds (4 mm diameter×4 mm thick), providing the necessary structural and mechanical environment for osteogenic differentiation, and cultured in bioreactors with medium perfusion. The interstitial flow velocity was set to a level necessary to maintain cell viability and function throughout the construct volume (400 μm/s), via enhanced mass transport. After 5 weeks of cultivation, the addition of osteogenic supplements (dexamethasone, sodium-β-glycerophosphate, and ascorbic acid-2-phosphate) to culture medium significantly increased the construct cellularity and the amounts of bone matrix components (collagen, bone sialoprotein, and bone osteopontin). Medium perfusion markedly improved the distribution of cells and bone matrix in engineered constructs. In summary, a combination of hASCs, decellularized bone scaffold, perfusion culture, and osteogenic supplements resulted in the formation of compact and viable bone tissue constructs.

Introduction

Skeletal defects due to trauma, tumors, infection, genetic diseases, and abnormal development often require bone transplantation. Following blood, this is the second most common tissue transplant, with 2.2 million grafting procedures performed annually worldwide. Because of the aging of the population, this number is expected to increase further in coming years. The preferred treatment option for bone repair is the use of autologous tissue, although the limited availability and donor site morbidity remain significant drawbacks to this method.[1,2] Tissue engineering could provide autologous bone tissue grafts formed by cells cultured on scaffolds and thereby alleviate the shortage of donor tissue. Human sources of osteogenic cells, appropriate scaffolds, bioreactor culture systems, and subsequent functional integration with the host are among the critical components for engineering viable bone grafts.

Human cells from a variety of tissues have been shown to have osteogenic potential, including osteoblasts,[3] mesenchymal stem cells (MSCs),[4,5] skin, amniotic membrane, lungs,[6] and adipose-derived stem cells (ASCs).[7,8] Human ASCs (hASCs) were selected for our study because of the ease of access of adipose tissue, high yield per unit tissue volume, rapid cell proliferation, and the possibility of either autologous or allogeneic use.[9] Osteogenic potential of these cells has been demonstrated in monolayer culture[7,8] and on various scaffolds including collagen,[10,11] akermanite,[12] poly(DL-lactic-*co*-glycolic acid),[13] and beta-tricalcium phosphate.[12,14] Animal studies have shown new bone formation by hASCs implanted subcutaneously[10,14–17] in calvarial defects[18,19] and mandibular defects.[20]

A scaffold is generally designed to provide a stimulatory three-dimensional environment for tissue formation.[11] A bone scaffold should be biocompatible and osteoinductive and have appropriate structural and mechanical properties.[1] Osteogenesis of human MSCs (hMSCs) cultured on scaffolds was enhanced by the presence of extracellular bone matrix.[21] Likewise, the implantation of engineered bone generated by the hMSCs enhanced bone healing *in vivo* when compared with the effects of either hMSC-seeded scaffold or scaffold alone.[22] Fully decellularized bone scaffolds were used in our study because of their ideal molecular composition, structural properties, and mechanical properties, enabling bone development *in vitro* and immediate mechanical support following graft implantation into load-bearing areas. Osteoinductive

[1]Department of Biomedical Engineering, Columbia University, New York, New York.
[2]Educell Ltd., Ljubljana, Slovenia.
[3]Pennington Biomedical Research Center, Louisiana State University System, Baton Rouge, Louisiana.

molecules (e.g., collagen and bone morphogenic proteins) that are preserved within the organic phase are potent modulators of osteogenic differentiation.[23,24] Scaffolds with pore sizes in the range of 200–900 μm[20,25–27] that mimic the structure of bone have been shown to enable cellular penetration, extracellular matrix production, and eventual blood vessel ingrowth.

In native bone, interstitial flow plays a major role in providing the exchange of nutrients, oxygen, and waste products with the metabolically active bone cells and it serves as a source of hydrodynamic shear that is an intrinsic component of the bone environment. In tissue engineering studies, medium perfusion enhanced the formation of bone from bone marrow-derived hMSCs.[5,28–31] Short-term perfusion of the stromal vascular fraction of human adipose tissue improved osteogenic and vasculogenic capabilities of the cells implanted *in vivo*.[32] When exposed to short-term fluid flow in parallel-plate flow chambers, ASCs responded in a similar fashion as bone cells.[33,34] As longer periods are needed for differentiation into a mature osteoblastic phenotype,[35] our study evaluated the effects of perfusion on ASC-based bone constructs for extended cultivation times.

We report here a promising novel approach for engineering bone tissue from hASCs cultured for 5 weeks on fully decellularized bone scaffolds in a perfusion bioreactor.

Materials and Methods

Isolation and expansion of hASCs

All protocols were reviewed and approved by the Pennington Biomedical Research Center Institutional Research Board. Liposuction aspirates from subcutaneous adipose tissue were obtained from four female donors (termed A, B, C, and D, without any identifiers) undergoing an elective procedure. hASCs were isolated from lipoaspirates using previously described methods[36] and expanded in high-glucose Dulbecco's modified Eagle's medium (DMEM) supplemented with 10% fetal bovine serum (FBS), 1 ng/mL basic fibroblast growth factor, and penicillin–streptomycin (1%). The cells were plated at a density of 5000 cells/cm^2 and expanded to the third passage that was used for all experiments performed in our study.

Phenotypic characterization of hASCs

Flow cytometric analysis of surface markers was carried out on cells at passage 0 for the presence of following antigens: CD29, CD34, CD44, CD45, CD73, CD90, and CD105, as previously described.[9,36]

Monolayer cultures

To test their osteogenic capacity, hASCs were plated at a density of 5000 cells/cm^2 and cultured in osteogenic medium consisting of high-glucose DMEM, FBS (10%), dexamethasone (100 nM), sodium-β-glycerophosphate (10 mM), ascorbic acid-2-phosphate (0.1 mM), and penicillin–streptomycin (1%). Control medium for cultivation of undifferentiated cells consisted of high-glucose DMEM, FBS (10%), and penicillin–streptomycin (1%). After 1–4 weeks of culture, $n = 3$–4 wells per condition and time points were assessed for alkaline phosphatase (AP), von Kossa staining, alizarin red, and DNA content.

Pellet cultures

Aliquots of 0.5×10^6 cells in suspension were centrifuged at 500 *g* for 12 min and incubated overnight to form round pellets of cells. Each pellet was cultured in a tube containing 1 mL of the control medium or osteogenic medium, for up to 4 weeks. For evaluation, the pellets were fixed in 10% formalin, dehydrated with graded ethanol washes, embedded in paraffin, sectioned to 5 μm, and mounted on glass slides. The sections were deparaffinized with Citrisolv (Fisher, Pittsburg, PA) and rehydrated with a graded series of ethanol washes. For von Kossa staining, the tissue sections were treated with 5% $AgNO_3$ and exposed to a strong light for 30 min to show mineral deposition, observed by black stain. Calcium and DNA contents were measured as described below.

Decellularized bone scaffolds

Scaffolds were decellularized as in our previous studies.[31] Briefly, trabecular bone pieces were cored from the carpometacarpal joints of young cows and washed with a high velocity stream of water to remove bone marrow. Scaffolds were further washed for 1 h in phosphate-buffered saline (PBS) with 0.1% ethylenediamine tetraacetic acid (EDTA) at room temperature, followed by sequential washes in hypotonic buffer (10 mM Tris and 0.1% EDTA) overnight at 4°C, in detergent (10 mM Tris and 0.5% sodium dodecyl sulfate [SDS]) for 24 h at room temperature, and in enzyme solution (50 U/mL DNAse, 1 U/mL RNAse, and 10 mM Tris) for 3 h at 37°C, to fully remove cellular material. Scaffolds were then rinsed in PBS, freeze-dried, and cut into 4 mm diameter×4 mm high cylindrical plugs. The densities of scaffolds were calculated based on the dry weights and exact dimensions. The scaffolds within the density range of 0.37–0.45 mg/mm^3 were selected for experiments and were sterilized in 70% ethanol.

Perfusion bioreactor

A novel perfusion bioreactor system has been used for culturing hASCs on decellularized bone scaffolds.[31] The culture medium (40 mL per bioreactor) flowed through a central port at the bottom of the bioreactor vessel from where it was evenly distributed into six channels leading into the individual culture wells. One scaffold per well was press-fit within a layer of polydimethylsiloxane. The medium from all six wells was then collected into the reservoir above the culture wells, where it was equilibrated with respect to oxygen and pH in a humidified incubator and exited through the port at the side of the bioreactor. For medium recirculation, a multichannel digital peristaltic pump (Ismatec; Cole-Parmer, Vernon Hills, IL) was used. The flow rate (1.8 mL/min, corresponding to the interstitial flow velocity of 400 μm/s through the scaffolds) was chosen based on previous experiments.[31]

Construct seeding and culture

Culture-expanded hASCs were suspended in control medium using 1.5×10^6 cells in 40 μL volume, and the cell suspension was added on the top of each blot-dried scaffold. The cell suspension was pipetted in and out, to enhance even distribution of cells within the scaffolds. After 15 min in the incubator, the scaffolds were flipped and an additional 10 μL of cell-free medium was added to the top to prevent them

from drying out. This process was repeated four times, after which the seeded constructs were transferred into six-well plates and incubated in control medium for 2 days to allow the cells to attach. Subsequently, $n = 9$ seeded scaffolds were used for evaluation of seeding efficiency; $n = 24$ scaffolds were transferred into four perfusion bioreactors (six per bioreactor); and $n = 24$ scaffolds were kept in static culture. Two types of medium (control and osteogenic) were used for both the static and bioreactor cultures.

The experimental groups were as follows: (1) static-control, (2) static-osteogenic, (3) perfused-control, and (4) perfused-osteogenic. In all groups, the culture medium was changed 50% twice weekly throughout the culture period. The scaffolds were harvested for assessments after 2 and 5 weeks of culturing. For DNA assays, $n = 3$ constructs per experimental group and time point were harvested, and another $n = 3$ constructs were used for histology, immunohistochemistry, scanning electron microscopy, and microcomputed tomography (μCT).

DNA content

The cells cultured in monolayers were washed with PBS, and then 200 μL of digestion buffer (10 mM Tris, 1 mM EDTA, 0.1% Triton X-100, 0.1 mg/mL proteinase K) was added and a cell scraper was used to remove the cells from the well. Cell pellets and tissue constructs were also washed in PBS and placed in 500 μL of digestion buffer in microcentrifuge tubes. All samples were incubated in digestion buffer overnight at 56°C. The supernatants were then drawn off and pipetted in duplicate in 96-well plates. Picogreen dye (Molecular Probes, Eugene, OR) was added to the samples in 1:1 ratio and read in a fluorescent plate reader (excitation 485 nm and emission 528 nm). A standard curve was prepared from a solution of salmon testes DNA (Molecular Probes). The conversion factor was obtained from initial studies to determine the DNA content of hASCs and corresponded to 5 pg DNA/cell.

Calcium assay

Cell pellets were extracted by 5% trichloroacetic acid (500 μL per sample). *O*-Cresolphtalein complex was added (Calcium CPC LiquiColor Test®; Stanbio Laboratory, Boerne, TX), and the calcium content was determined spectrophotometrically at 550 nm.

Live/dead assay

The constructs were cut in half, incubated with calcein AM (indicating live cells) and ethidium homodimer-1 (indicating dead cells) according to the manufacturer's protocol (LIVE/DEAD® Viability/Cytotoxicity Kit; Molecular Probes), and then observed and imaged on a confocal microscope. Optical slices were taken from the surface at 10 μm intervals, up to the depth of 160 μm, and then presented as a vertical projection.

AP assay

The cells were harvested in 100 μL of lysate buffer (PBS, 1% Triton X-100, 0.5% sodium deoxycholate, 0.1% SDS, 0.1 mg/mL phenylmethylsulfonylfluoride, and 0.3% aprotinin), maintained on ice, and vortexed intermittently for 30 min to break down the cell membranes. The extracts were removed and centrifuged and the supernatants were stored at −20°C. Fifty microliters of a sample was incubated with 50 μL alkaline buffer and 50 μL nitrophenyl-phosphate substrate solution in microcentrifuge tubes at 37°C for 15 min. The reaction was stopped with 0.5 N NaOH. The absorbance was read at 405 nm and compared with a standard curve obtained from *p*-nitrophenol solutions of known concentrations.

Alizarin red assay

The cultures were fixed in 70% ethanol for 1 h at 4°C, rinsed three times with distilled water, and stained in 2% alizarin red solution (dissolved in distilled water) for 10 min at room temperature. The wells were rinsed five times with distilled water and photographed using phase-contrast microscopy. The alizarin red stain was eluted by incubation in 10% cetylpyridinium chloride monohydrate (dissolved in distilled water) for 30 min, and the dye was quantified by absorption at OD_{540}.[7]

Histology and immunohistochemistry

The constructs were washed in PBS and fixed in 10% formalin for 1 day, decalcified with immunocal solution (Decal Chemical, Tallman, NY) for 1 day, dehydrated with graded ethanol washes, embedded in paraffin, sectioned to 5 μm, and mounted on glass slides. The sections were deparaffinized with Citrisolv, rehydrated with a graded series of ethanol washes, and then stained for total collagen using Trichrome stainings. 4′-6-Diamidino-2-phenylindole staining was performed to observe nuclei.

The staining for bone sialoprotein (BSP) and osteopontin (OP) was carried out as follows: the rehydrated sections were blocked with normal serum, stained sequentially with primary antibodies (BSP: rabbit polyclonal anti-BSP II [AB1854; Chemicon, Temecula, CA], and OP: rabbit polyclonal anti-OP [AB1870; Chemicon]) and secondary antibody, and developed with a biotin/avidin system. The serum, secondary antibody, and developing reagents were obtained from Vector Laboratories (Burlington, CA) and included in the Vector Elite ABC kit (universal) (PK6200) and DAB/Ni Substrate (SK-4100). Negative controls were performed by omitting the primary antibody incubation step.

Scanning electron microscopy

Samples were washed in PBS, fixed in 2% glutaraldehyde in sodium cacodylate buffer for 2 h, washed in buffer, and freeze-dried overnight in a lyophillizer. Before imaging, samples were coated with gold/palladium. The inner and outer surfaces of the construct were imaged.

Microcomputed tomography

μCT was performed using a modified version of a previously established protocol.[37] Samples were aligned along their axial direction and stabilized with wet gauze in a 15 mL centrifuge tube. The tube was clamped in the specimen holder of a vivaCT 40 system (SCANCO Medical AG, Basserdorf, Switzerland). The 4 mm length of the scaffold was scanned at 21 μm isotropic resolution. The bone volume (BV) was obtained from the application of a global thresholding technique so that only the mineralized tissue is detected. The BV fraction was calculated as the fraction of measured BV per unit sample volume.

Statistical analysis

Data are presented as average ± standard deviation. Statistical significance was determined using *t*-test and analysis of variance followed by Tukey's *post hoc* analysis, using STATISTICA software (StatSoft, Tulsa, OK). $p < 0.05$ was considered significant.

Results

Osteogenic characteristics of culture-expanded hASCs: Effects of medium composition and donor-to-donor variability

Primary hASCs were characterized by fluorescence-activated cell sorting analysis to determine the presence of the following antigens: CD29 (98.9%), CD34 (92.3%), CD44 (24.3%), CD45 (12.1%), CD73 (79.0%), CD90 (94.9%), and CD105 (98.0%) (Fig. 1A). Quantitative biochemical assay showed significantly higher amounts of AP in osteogenic than in control cultures of hASCs ($p < 0.05$) at all time points during cultivation (weeks 1–4) (Fig. 1B). Staining with alizarin red and von Kossa for mineral deposition corroborated this finding (Supplemental Fig. S1, available online at www.liebertonline.com).

The measurement of calcium levels in pellets of cells obtained from four different donors (A, B, C, and D) and cultured for 4 weeks in osteogenic or control medium showed that osteogenic culture conditions resulted in significantly higher ($p < 0.001$) levels of calcium (Fig. 1C) and markedly stronger alizarin red staining (Supplemental Fig. S1). Strong mineral deposition after 4 weeks of culture under osteogenic conditions was confirmed by von Kossa staining of both monolayer cultures (Fig. 1E) and pellet cultures for all four donors tested (Fig. 1D, F, G, H). The control samples cultured in unsupplemented medium were negative (insets in Fig. 1D–H). Collectively, these data show strong effects of osteogenic supplements and time of culture, and a significant donor-to-donor variability in the osteogenesis of hASCs.

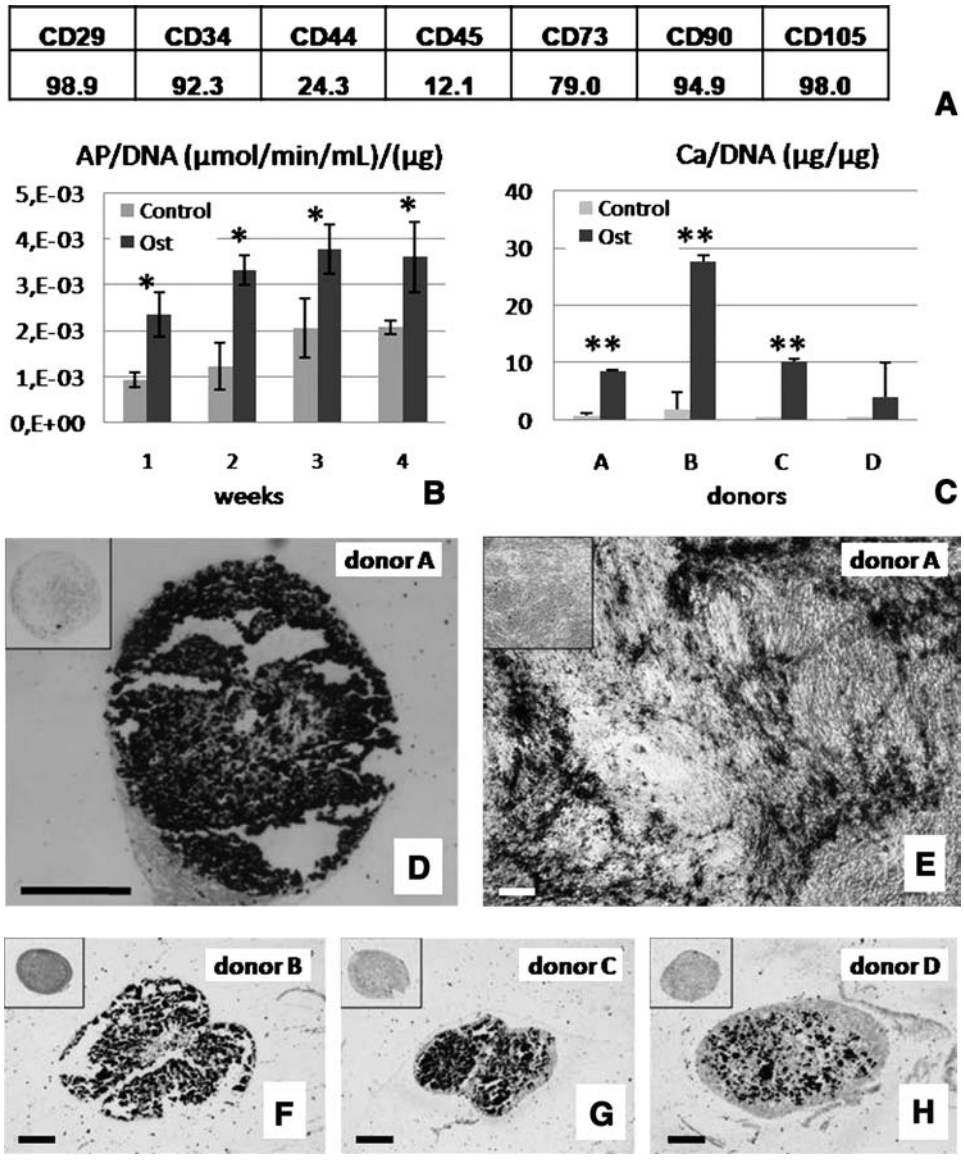

FIG. 1. Osteogenic capacity of human adipose-derived stem cells (hASCs). (**A**) The presence of antigens in the starting population of hASCs. (**B**) Alkaline phosphatase activity of hASCs was higher in osteogenic (Ost) than in unsupplemented control medium (Control) (data are shown for donor A, $n = 3$, $^{*}p < 0.05$). (**C**) Calcium contents of hASC pellets from four different donors (A, B, C, and D) cultured in osteogenic medium (Ost) and control medium (Control) ($n = 3$–4, $^{**}p < 0.001$). (**D, F–H**) von Kossa staining of the central regions of osteoinduced pellets of donors A, B, C, and D (black: calcium deposits). Insets show negative stains for pellets cultured in control medium. (**E**) von Kossa staining of osteoinduced cell monolayers for donor A is shown for comparison. Scale bar is 250 µm for all images.

Cell viability and distribution: Effects of medium composition and medium perfusion

The efficiency of cell seeding, calculated as a fraction of the initial cells detected in the scaffold after seeding, was $73\% \pm 14\%$. Bioreactor cultivation enabled uniform flow of medium through six constructs simultaneously (Fig. 2A, B). Only viable cells were observed in all samples and at all time points throughout the 5 weeks of culture (Fig. 2C, where green stain indicates live cells in representative samples cultured for 5 weeks in perfusion or statically). This result was obtained for both construct culture groups and both media compositions (Supplemental Fig. S2, available online at www.liebertonline.com).

DNA assay demonstrated that cell proliferation occurred mostly during the first 2 weeks of cultivation (Fig. 2D). At the end of culture, cell numbers were significantly higher for samples cultured in osteogenic when compared with control medium ($p < 0.05$), for all types of cell culture: monolayers (3.7-fold), pellets (2-fold), statically cultured constructs (1.5-fold), and constructs cultured with perfusion (2.5-fold) (Fig. 2E). Parallel differentiation studies of hMSCs derived from bone marrow aspirates showed the levels of differentiation markers comparable to those of hASCs (data not shown).

Distribution of bone tissue matrix: Effects of medium perfusion and medium composition

4′-6-Diamidino-2-phenylindole staining showed striking differences in cell distribution between constructs cultured statically compared with those cultured with medium perfusion. Homogenously seeded scaffolds (Fig. 3A) that were subsequently cultured statically in osteogenic medium for 5 weeks contained cells mostly within a thin peripheral region of the construct (Fig. 3B). In contrast, in the matching constructs cultured with perfusion, cells were distributed throughout the entire construct volume (Fig. 3C). The formation of collagen matrix was observed predominantly at the periphery of statically cultured constructs and throughout perfused constructs (Fig. 3E–F). Notably, the regions with

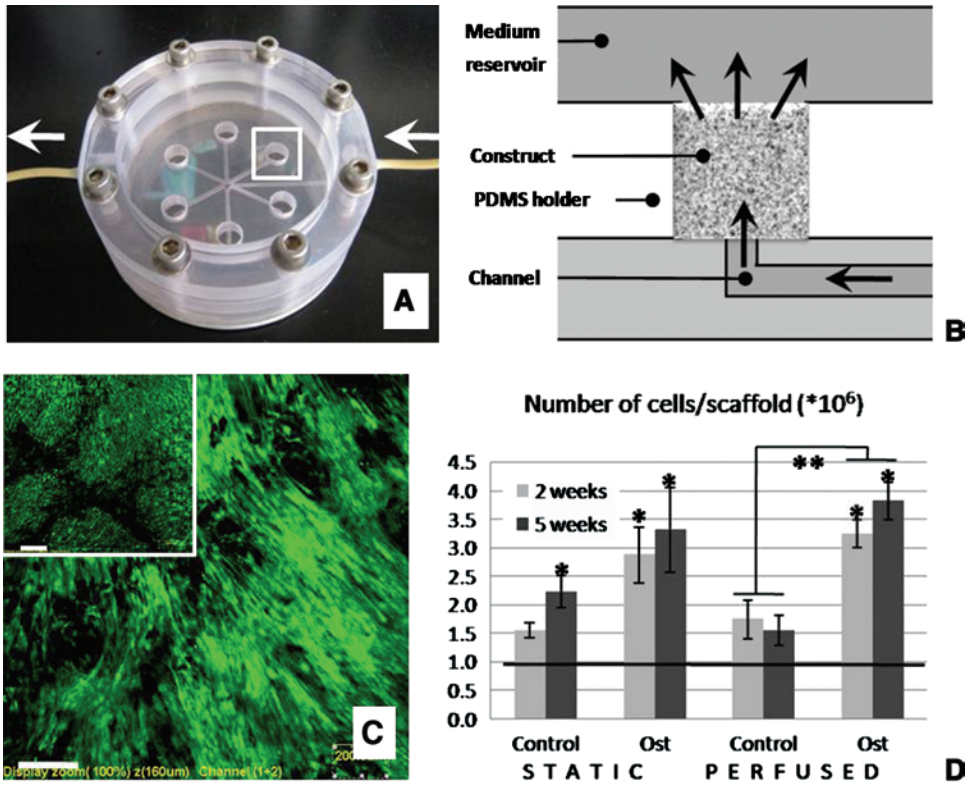

Type of culture		Number of cells (*10^6) ± SD	Fold difference
Pellets	Control	0.13 ± 0.05	2.0 (p<0.05)
	Ost	0.27 ± 0.03	
Monolayers	Control	27.46 ± 0.56	3.7 (p<0.05)
	Ost	101.41 ± 3.46	
Constructs (static)	Control	2.22 ± 0.28	1.5
	Ost	3.31 ± 0.74	
Constructs (perfused)	Control	1.55 ± 0.27	2.5 (p<0.05)
	Ost	3.82 ± 0.33	

E

FIG. 2. Cell content and viability during 5 weeks of culture: four culture settings and two culture media. (**A**) Perfusion bioreactor used in the study enables culturing of six constructs simultaneously. The region indicated by a white rectangle is shown in panel B in full detail. Arrows indicate directions of medium flow. (**B**) Medium flows throughout the scaffold, as indicated by arrows. The schematic corresponds to the region indicated by rectangle in the figure A. (**C**) After 5 weeks of culture, tissue constructs from both the perfused and static groups (inset) contained viable cells. Live/dead assay of the central regions of the constructs is shown (green indicates live cells and red would indicate dead cells). Scale bar is 200 μm. (**D**) The number of cells in constructs increased up to three times during the culture period in comparison to the initial cell numbers (denoted by a line) ($n = 3$, $^*p < 0.05$). Osteogenic medium resulted in higher amounts of cells than control medium ($^{**}p < 0.05$). (**E**) Number of cells was higher under osteogenic conditions when compared with control conditions in all types of cultures performed. Color images available online at www.liebertonline.com/ten.

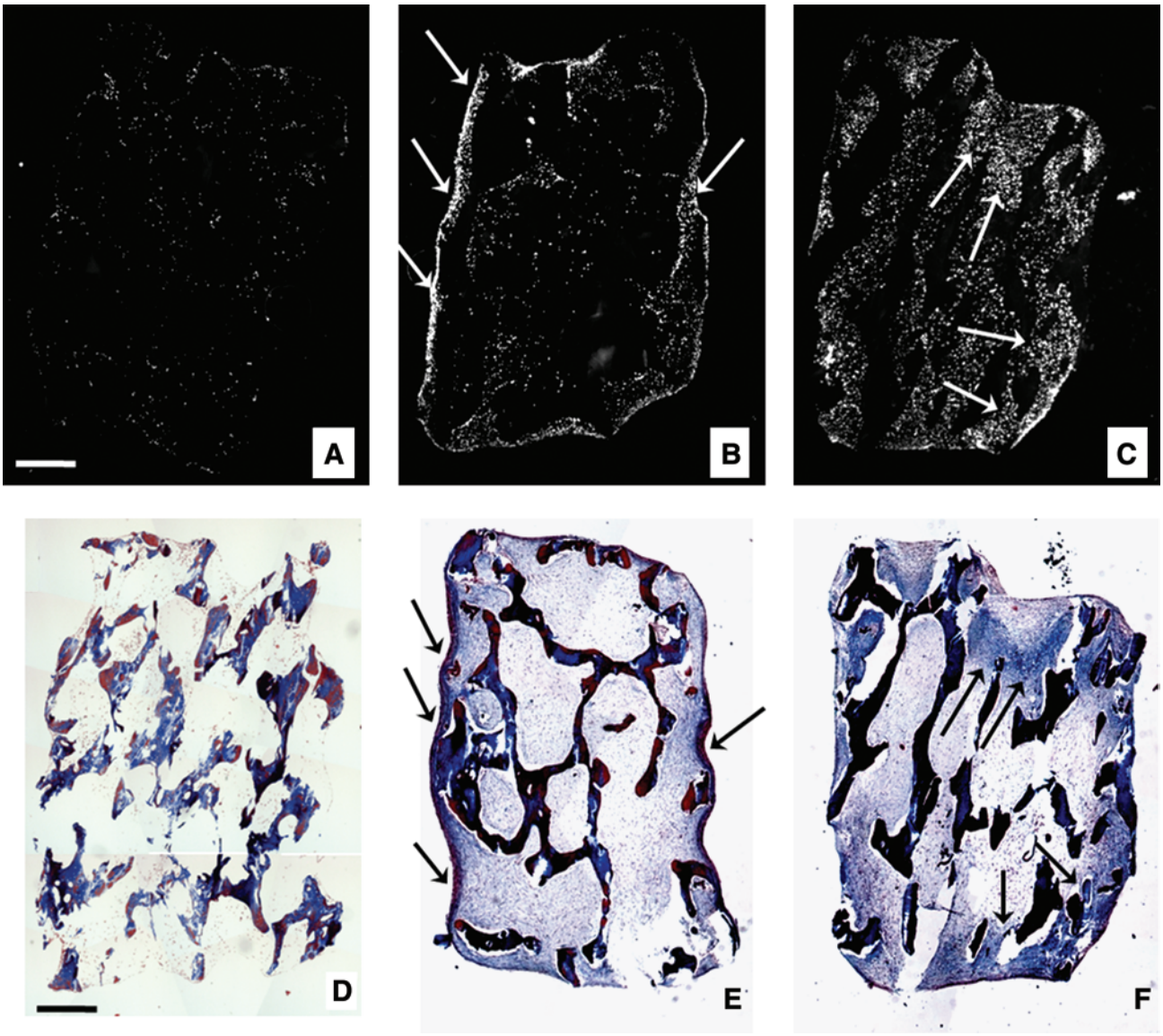

FIG. 3. Cell and matrix distribution within constructs: effects of perfusion. Constructs immediately after seeding (**A, D**), and after 5 weeks of culture in osteogenic medium under either static conditions (**B, E**) or with medium perfusion (**C, F**). Constructs were stained with (**A–C**) 4′-6-diamidino-2-phenylindole to visualize cell distribution (cells shown in white) and (**D–F**) trichrome to observe the presence of collagen-rich matrix (blue). (**A**) Seeding resulted in even initial distribution of cells throughout the scaffold. After 5 weeks of static culture, cells were found mostly in the outer regions of the constructs (**B**). After 5 weeks of culture with medium perfusion, cells were evenly distributed throughout the construct volume (**C**). After 5 weeks of culture, the regions of newly formed collagen matrix (indicated by arrows in **E** and **F**) colocalized with the regions of higher cell densities (indicated by arrows in **B** and **C**). Scale bar: 0.5 mm (**A, D**). Color images available online at www.liebertonline.com/ten.

high cell density (Fig. 3B, C) colocalized with the regions containing high amounts of new collagen matrix (Fig. 3E, F).

Constructs cultured in control medium in either static or perfused culture displayed no presence of either BSP (Fig. 4A, E) or bone OP. In osteogenic medium, collagen and OP were detected after 2 weeks of culture (data not shown). After 5 weeks of culture, statically cultured constructs showed deposition of BSP (Fig. 4B), OP (Fig. 4C), and collagen (Fig. 4D) in the outer but not inner regions of the constructs. In contrast, constructs cultured with perfusion exhibited uniform spatial distributions of all three proteins (Fig. 4F–H).

Mineralization of perfused constructs was monitored using μCT, to determine that the BV fraction increased by 8% after 5 weeks of cultivation with medium perfusion (Fig. 5A, B). Scanning electron microscopy images show that cells and deposited matrix filled out pore spaces in the outer (Fig. 5C, D) as well as in inner construct regions (Fig. 5E, F) and that small round crystals formed at construct surfaces (Fig. 5D).

Discussion

In this study, we investigated the capacity of hASCs to form bone grafts when cultured on scaffolds made of decellularized

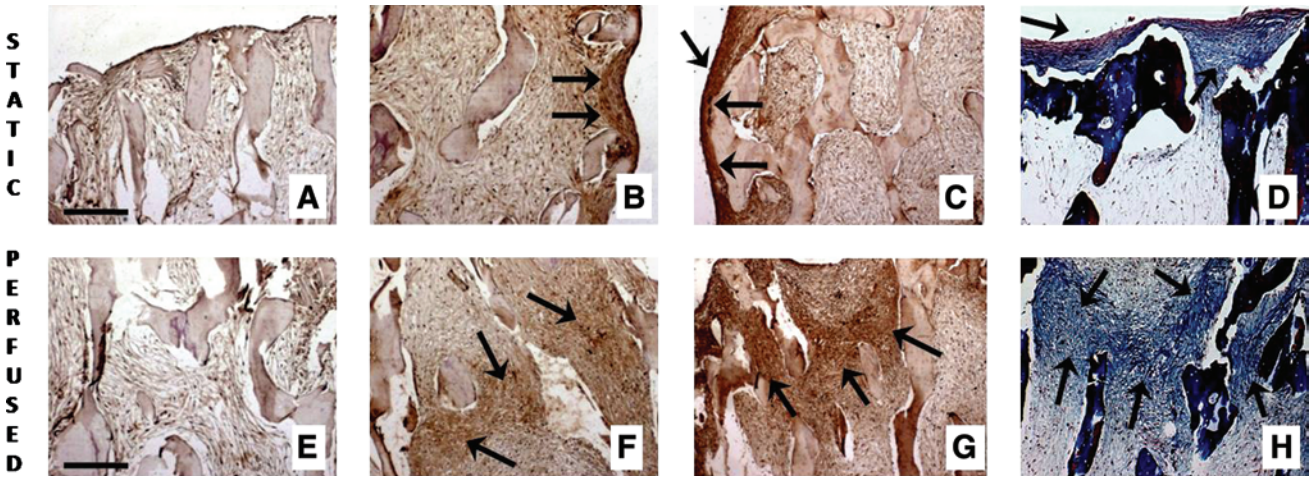

FIG. 4. Presence of collagen, bone sialoprotein (BSP), and osteopontin within the hASCs constructs. Absence of osteogenic supplements resulted in lack of bone matrix markers in static as well as in perfused cultures: result for BSP is shown (**A, E**). Deposition of BSP (**B, F**), osteopontin (**C, G**), and collagen (**D, H**) in constructs cultured for 5 weeks under osteogenic conditions, either statically (**B–D**) or with medium perfusion (**F–H**). Strong presence of all three bone markers (indicated by arrows) was observed throughout the perfused constructs (central regions are shown in **F, G, H**) and only at the periphery of statically cultured constructs (construct edges are shown in **B, C, D**). Scale bar: 250 μm (**A, E**). Color images available online at www.liebertonline.com/ten.

bone, with perfusion of culture medium containing osteogenic supplements. Previously published studies documented the osteogenic potential of hASCs in static culture on a variety of scaffolds.[10–14,38] However, little is known about the effects of perfusion (interstitial flow) on spatial distribution of these cells and the formation of bone during prolonged culture. We have previously shown that hMSCs derived from bone marrow aspirates could be induced to proliferate and form spatially uniform bone on decellularized bone scaffolds if cultured with medium perfusion.[31] Although some studies suggested that

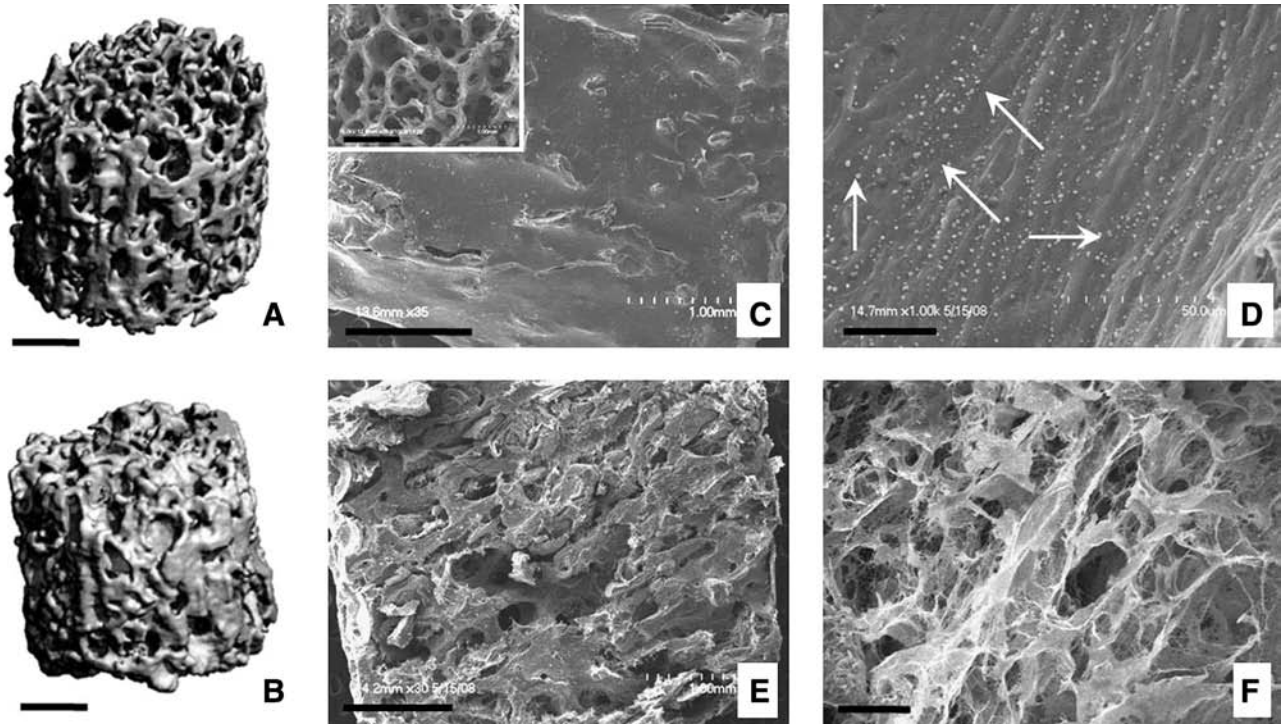

FIG. 5. Morphology and mineral content of tissue constructs cultured with perfusion of osteogenic medium. Microcomputed tomography images of the initial (unseeded) scaffold (**A**) and a tissue construct cultured for 5 weeks (**B**) show the new mineral deposition during cultivation. Scanning electron microscopy images (**C–F**) show that cells and deposited matrix filled the pore spaces of initial scaffold (inset in **C**), both in the outer (**C, D**) and the inner construct regions (**E, F**). Small round formations (arrows in **D**) are consistent with the formation of hydroxyapatite crystals (**D**). Scale bar: 1 mm (**A, B, C, E**) and 25 μm (**D, F**).

hASCs may be less suitable for bone tissue engineering than hMSCs,[39] our study suggested similar differentiation capabilities of hASCs and hMSCs for bone formation.[5,31,40]

The starting hASCs (passage 0) were characterized by flow cytometric analysis of surface antigens (Fig. 1A) to assess the initial levels of marker expression for various donors. In an earlier study that we conducted with hASCs, the expression patterns for mesenchymal cell markers (CD105, CD73, and CD90) stayed consistently high over several passages in monolayer culture.[9] However, we also tested the expanded hASCs (passage 3) for osteogenic differentiation using biochemical assays and immunostains to further address the donor-to-donor variability and confirm the ability of passaged cells for osteogenic differentiation (Fig. 1C–H and Supplemental Fig. S1).

Decellularized bone scaffolds supported the attachment and proliferation of hASCs, in a manner similar to that shown previously for hMSCs[31]; however, hASC-based constructs yielded five times higher cellularity after 5 weeks of cultivation starting from the same initial seeding densities.

With respect to the presence of live cells only within the peripheral 200–300 μm thick layer shown in previous studies,[27] we observed live cells at millimeter depths in all culture groups (Fig. 3B, C, E, F). The outer construct regions contained a dense layer of cells, as in previous studies of alveolar osteoblasts,[41] calvarial osteoblasts,[27] and rat MSCs.[42] Notably, the formation of an outer layer of cells can additionally contribute to insufficient nutrient–waste exchange in the construct interior. Further studies in our lab as well as reports in the literature[43,44] indicate that hypoxia negatively affects osteogenic differentiation of hASCs. Thus, insufficient oxygenation in the central construct regions could correlate with the nonuniform differentiation of cells and result in nonuniform bone matrix deposition. In contrast, medium perfusion enabled the cultivation of large constructs with spatially uniform distributions of cells, consistent with our previous studies of hMSC-based bone constructs.[31] Improved cell distribution in perfusion culture was also shown for other tissue engineering systems with medium perfusion.[28–30] In general, uniform cell distribution is an important factor for uniform formation of the bone matrix.[20,38]

Cell densities observed in perfused constructs engineered in this study (~76 million cells/cm^3 scaffold volume, based on DNA assay) are lower than those in native cancellous bone (~500 million cells/cm^3).[45] Nevertheless, these values are 3–10 times higher than cell densities in tissue-engineered bone grafts cultured under perfusion that have been reported thus far: 24 million cells/cm^3,[28] 19 million cells/cm^3,[29] 15 million cells/cm^3,[31] or 7 million cells/cm^3.[30]

Interestingly, the presence of osteogenic supplements consistently resulted in higher proliferation of hASCs in all culture models (monolayer, pellet, static, and perfused constructs culture; Fig. 2E), which could be of importance in clinical applications where high cell numbers are needed. The same trend was observed in studies using hMSCs[4] and rabbit ASCs[46]; however, it contrasts the findings with rat MSCs.[47]

Ascorbic acid, besides its role in collagen production,[48] is a potent positive modulator of hMSC[49] and hASC[50] proliferation. In contrast, both increases[51] and decreases[47] in cell proliferation have been associated with the use of dexamethasone in culture medium. Decellularized bone scaffolds did not induce bone matrix deposition by hASCs in the absence of osteogenic supplements (Fig. 1A, E), consistent with nonosteoinductive properties of the scaffolds observed *in vivo*.[52] It has also been suggested that partial matrix demineralization might be necessary for osteoinductive factors to become accessible to the cells.[53] Further, the use of SDS in the process of decelullarization has been shown to affect the biochemical composition of native scaffolds (reduction of glycosaminoglycan content and collagen disruption) in anterior cruicate ligament[54]; therefore, it might have similar effects in bone matrix. Although bovine bone has been used as a scaffold in our study, human bone source could be considered for actual clinical applications. We are now working on the design of synthetic scaffolds mimicking the structure and mechanical properties of decellularized native bone, and this may be an attractive off the shelf alternative to the use of decellularized human bone.

hASC proliferation and osteogenesis was in agreement with the known sequence of *in vitro* osteoblast development and maturation.[35] Collagen is the major organic component of the bone matrix and is secreted by osteoblasts during early osteoblastic differentiation before matrix calcification.[55] Subsequently, cells stop proliferating and start to deposit OP and BSP, both being markers of the final-mineralization phase in osteoblast development.[35] The presence of newly formed mineral in constructs additionally confirmed mature osteoblast-like characteristics of hASC constructs (Fig. 5B).

The regions with newly deposited bone matrix, rich in collagen, BSP, and OP, colocalized with regions of high cell density (Fig. 3), suggesting that high cell densities enhance bone matrix production, as during the normal developmental sequence, where mesenchymal condensation precedes ossification. Additional supporting evidence for the beneficial role of high cell density on osteogenic differentiation is the stronger mineralization (noted by von Kossa staining) of the cells in pellet cultures compared with monolayer cultures (Fig. 1D, E). In pellet cultures, close proximity of the cells and a three-dimensional environment contribute to osteogenic differentiation.

Perfused constructs displayed more uniform distributions of bone matrix than statically cultured constructs. Improved nutrient exchange and shear stress induced by medium flow have been shown to account for improved osteogenic phenotype in MSCs.[28–31] In our system, medium flow alone, without osteogenic supplements, was not sufficient to induce osteogenic differentiation in hASCs. This might be due to the insufficient magnitude of shear stress, different nature of the stimulus (steady, unidirectional shear vs. oscillating flow), or the fact that ASCs need a certain extent of osteogenic predifferentiation before they can show response to shear stress.[33] It should be noted that the shear stress values in our system were of the order of 0.01 Pa,[31] whereas a mean shear stress of 0.6 Pa of pulsating fluid flow was reported to induce bone-like responsiveness for ASCs in two-dimensional parallel-plate flow chamber.[33,34]

In summary, perfusion culture of hASCs on decellularized bone scaffolds in the presence of osteogenic supplements resulted in millimeters thick, viable bone-like constructs, with strong expression of osteoblastic phenotype. Osteogenic supplements significantly increased construct cellularity, and

the perfusion markedly improved the amounts and distributions of cells and bone matrix. Our model provides a starting point to engineer bone constructs for potential clinical use, as the hASCs are an easily accessible cell source, the decellularized bone scaffolds provide mechanical stability, and the bioreactor culture assures proper maturation of bone grafts. One of the main challenges is the survival of these highly cellular constructs after implantation; therefore, suitable ways of vascularization should be explored. hASC-based grafts can also serve as tools for bone disease or development studies.

Acknowledgments

The authors are grateful to Leo Q. Wan, Supansa Yodmuang, and Sarindr Bhumiratana for their help with experiments; Elizabeth Clubb and James Wade for providing liposuction aspirates; and Gang Yu and Xiying Wu for help with cell isolation and characterization. The work was supported in part by NIH (P41-EB002520 and R01-DE16525 to G.V.N., and P30 DK072476 to J.M.G.), the Pennington Biomedical Research Foundation (to J.M.G.), and the Ministry of Higher Education, Science, and Technology of Slovenia (3311-04-831828).

Disclosure Statement

All authors have no conflict of interests.

References

1. Salgado, A.J., Coutinho, O.P., and Reis, R.L. Bone tissue engineering: state of the art and future trends. Macromol Biosci **4,** 743, 2004.
2. Giannoudis, P.V., Dinopoulos, H., and Tsiridis, E. Bone substitutes: an update. Injury **36,** 20, 2005.
3. Lecanda, F., Avioli, L.V., and Cheng, S.L. Regulation of bone matrix protein expression and induction of differentiation of human osteoblasts and human bone marrow stromal cells by bone morphogenetic protein-2. J Cell Biochem **67,** 386, 1997.
4. Bruder, S.P., Jaiswal, N., and Haynesworth, S.E. Growth kinetics, self-renewal, and the osteogenic potential of purified human mesenchymal stem cells during extensive subcultivation and following cryopreservation. J Cell Biochem **64,** 278, 1997.
5. Meinel, L., Karageorgiou, V., Fajardo, R., Snyder, B., Shinde-Patil, V., Zichner, L., Kaplan, D., Langer, R., and Vunjak-Novakovic, G. Bone tissue engineering using human mesenchymal stem cells: effects of scaffold material and medium flow. Ann Biomed Eng **32,** 112, 2004.
6. Sudo, K., Kanno, M., Miharada, K., Ogawa, S., Hiroyama, T., Saijo, K., and Nakamura, Y. Mesenchymal progenitors able to differentiate into osteogenic, chondrogenic, and/or adipogenic cells *in vitro* are present in most primary fibroblast-like cell populations. Stem Cells **25,** 1610, 2007.
7. Halvorsen, Y.D.C., Franklin, D., Bond, A.L., Hitt, D.C., Auchter, C., Boskey, A.L., Paschalis, E.P., Wilkison, W.O., and Gimble, J.M. Extracellular matrix mineralization and osteoblast gene expression by human adipose tissue-derived stromal cells. Tissue Eng **7,** 729, 2001.
8. Zuk, P.A., Zhu, M., Mizuno, H., Huang, J., Futrell, J.W., Katz, A.J., Benhaim, P., Lorenz, H.P., and Hedrick, M.H. Multilineage cells from human adipose tissue: implications for cell-based therapies. Tissue Eng **7,** 211, 2001.
9. Mitchell, J.B., McIntosh, K., Zvonic, S., Garretta, S., Floyd, Z.E., Kloster, A., Di Halvorsen, Y., Storms, R.W., Goh, B., Kilroy, G., Wu, X.Y., and Gimble, J.M. Immunophenotype of human adipose-derived cells: temporal changes in stromal-associated and stem cell-associated markers. Stem Cells **24,** 376, 2006.
10. Kakudo, N., Shimotsuma, A., Miyake, S., Kushida, S., and Kusumoto, K. Bone tissue engineering using human adipose-derived stem cells and honeycomb collagen scaffold. J Biomed Mater Res A **84A,** 191, 2008.
11. Gabbay, J.S., Heller, J.B., Mitchell, S.A., Zuk, P.A., Spoon, D.B., Wasson, K.L., Jarrahy, R., Benhaim, P., and Bradley, J.P. Osteogenic potentiation of human adipose-derived stem cells in a 3-dimensional matrix. Ann Plast Surg **57,** 89, 2006.
12. Liu, Q., Cen, L., Yin, S., Chen, L., Liu, G., Chang, J., and Cui, L. A comparative study of proliferation and osteogenic differentiation of adipose-derived stem cells on akermanite and beta-TCP ceramics. Biomaterials **29,** 4792, 2008.
13. Lee, J.H., Rhie, J.W., Oh, D.Y., and Ahn, S.T. Osteogenic differentiation of human adipose tissue-derived stromal cells (hASCs) in a porous three-dimensional scaffold. Biochem Biophys Res Commun **370,** 456, 2008.
14. Hattori, H., Masuoka, K., Sato, M., Ishihara, M., Asazuma, T., Takase, B., Kikuchi, M., and Nemoto, K. Bone formation using human adipose tissue-derived stromal cells and a biodegradable scaffold. J Biomed Mater Res B Appl Biomater **76B,** 230, 2006.
15. Lee, J.A., Parrett, B.M., Conejero, J.A., Laser, J., Chen, J., Kogon, A.J., Nanda, D., Grant, R.T., and Breitbart, A.S. Biological alchemy: engineering bone and fat from fat-derived stem cells. Ann Plast Surg **50,** 610, 2003.
16. Justesen, J., Pedersen, S.B., Stenderup, K., and Kassem, M. Subcutaneous adipocytes can differentiate into bone-forming cells *in vitro* and *in vivo*. Tissue Eng **10,** 381, 2004.
17. Hicok, K.C., Du Laney, T.V., Zhou, Y.S., Halvorsen, Y.D.C., Hitt, D.C., Cooper, L.F., and Gimble, J.M. Human adipose-derived adult stem cells produce osteoid *in vivo*. Tissue Eng **10,** 371, 2004.
18. Dudas, J.R., Marra, K.G., Cooper, G.M., Penascino, V.M., Mooney, M.P., Jiang, S., Rubin, J.P., and Losee, J.E. The osteogenic potential of adipose-derived stem cells for the repair of rabbit calvarial defects. Ann Plast Surg **56,** 543, 2006.
19. Cowan, C.M., Shi, Y.Y., Aalami, O.O., Chou, Y.F., Mari, C., Thomas, R., Quarto, N., Contag, C.H., Wu, B., and Longaker, M.T. Adipose-derived adult stromal cells heal critical-size mouse calvarial defects. Nat Biotechnol **22,** 560, 2004.
20. Abukawa, H., Shin, M., Williams, W.B., Vacanti, J.P., Kaban, L.B., and Troulis, M.J. Reconstruction of mandibular defects with autologous tissue-engineered bone. J Oral Maxillofac Surg **62,** 601, 2004.
21. Datta, N., Holtorf, H.L., Sikavitsas, V.I., Jansen, J.A., and Mikos, A.G. Effect of bone extracellular matrix synthesized *in vitro* on the osteoblastic differentiation of marrow stromal cells. Biomaterials **26,** 971, 2005.
22. Meinel, L., Fajardo, R., Hofmann, S., Langer, R., Chen, J., Snyder, B., Vunjak-Novakovic, G., and Kaplan, D. Silk implants for the healing of critical size bone defects. Bone **37,** 688, 2005.

23. Wang, J., Yang, R., Gerstenfeld, L.C., and Glimcher, M.J. Characterization of demineralized bone matrix-induced osteogenesis in rat calvarial bone defects: III. Gene and protein expression. Calcif Tissue Int **67,** 314, 2000.
24. Swoboda, H.F., Wimmer, F.M., Pfeiffer, K., and Schmidt, K.H. Ectopic bone induction by partially purified bone extract alone or attached to biomaterials. Biomater Artif Cells Artif Organs **18,** 383, 1990.
25. Burg, K.J.L., Porter, S., and Kellam, J.F. Biomaterial developments for bone tissue engineering. Biomaterials **21,** 2347, 2000.
26. Logeart-Avramoglou, D., Anagnostou, F., Bizios, R., and Petite, H. Engineering bone: challenges and obstacles. J Cell Mol Med **9,** 72, 2005.
27. Ishaug-Riley, S.L., Crane-Kruger, G.M., Yaszemski, M.J., and Mikos, A.G. Three-dimensional culture of rat calvarial osteoblasts in porous biodegradable polymers. Biomaterials **19,** 1405, 1998.
28. Bancroft, G.N., Sikavitsast, V.I., van den Dolder, J., Sheffield, T.L., Ambrose, C.G., Jansen, J.A., and Mikos, A.G. Fluid flow increases mineralized matrix deposition in 3D perfusion culture of marrow stromal osteloblasts in a dose-dependent manner. Proc Natl Acad Sci USA **99,** 12600, 2002.
29. Sikavitsas, V.I., Bancroft, G.N., Holtorf, H.L., Jansen, J.A., and Mikos, A.G. Mineralized matrix deposition by marrow stromal osteoblasts in 3D perfusion culture increases with increasing fluid shear forces. Proc Natl Acad Sci USA **100,** 14683, 2003.
30. Gomes, M.E., Sikavitsas, V.I., Behravesh, E., Reis, R.L., and Mikos, A.G. Effect of flow perfusion on the osteogenic differentiation of bone marrow stromal cells cultured on starch-based three-dimensional scaffolds. J Biomed Mater Res A **67A,** 87, 2003.
31. Grayson, W.L., Bhumiratana, S., Cannizzaro, C., Chao, P.H., Lennon, D.P., Caplan, A.I., and Vunjak-Novakovic, G. Effects of initial seeding density and fluid perfusion rate on formation of tissue-engineered bone. Tissue Eng A **14,** 1809, 2008.
32. Scherberich, A., Galli, R., Jaquiery, C., Farhadi, J., and Martin, I. Three-dimensional perfusion culture of human adipose tissue-derived endothelial and osteoblastic progenitors generates osteogenic constructs with intrinsic vascularization capacity. Stem Cells **25,** 1823, 2007.
33. Knippenberg, M., Helder, M.N., Doulabi, B.Z., Semeins, C.M., Wuisman, P., and Klein-Nulend, J. Adipose tissue-derived mesenchymal stem cells acquire bone cell-like responsiveness to fluid shear stress on osteogenic stimulation. Tissue Eng **11,** 1780, 2005.
34. Tjabringa, G.S., Vezeridis, P.S., Zandieh-Doulabi, B., Helder, M.N., Wuisman, P., and Klein-Nulend, J. Polyamines modulate nitric oxide production and COX-2 gene expression in response to mechanical loading in human adipose tissue-derived mesenchymal stem cells. Stem Cells **24,** 2262, 2006.
35. Lian, J.B., and Stein, G.S. Development of the osteoblast phenotype: molecular mechanisms mediating osteoblast growth and differentiation. Iowa Orthop J **15,** 118, 1995.
36. McIntosh, K., Zvonic, S., Garrett, S., Mitchell, J.B., Floyd, Z.E., Hammill, L., Kloster, A., Halvorsen, Y.D., Ting, J.P., Storms, R.W., Goh, B., Kilroy, G., Wu, X.Y., and Gimble, J.M. The immunogenicity of human adipose-derived cells: temporal changes *in vitro*. Stem Cells **24,** 1246, 2006.
37. Liu, X.S., Sajda, P., Saha, P.N., Wehrli, F.W., and Guo, X.E. Quantification of the roles of trabecular microarchitecture and trabecular type in determining the elastic modulus of human trabecular bone. J Bone Miner Res **21,** 1608, 2006.
38. Hao, W., Hu, Y.Y., Wei, Y.Y., Pang, L., Lv, R., Bai, J.P., Xiong, Z., and Jiang, M. Collagen I gel can facilitate homogenous bone formation of adipose-derived stem cells in PLGA-beta-TCP scaffold. Cells Tissues Organs **187,** 89, 2008.
39. Im, G.I., Shin, Y.W., and Lee, K.B. Do adipose tissue-derived mesenchymal stem cells have the same osteogenic and chondrogenic potential as bone marrow-derived cells? Osteoarthritis Cartilage **13,** 845, 2005.
40. Marolt, D., Augst, A., Freed, L.E., Vepari, C., Fajardo, R., Patel, N., Gray, M., Farley, M., Kaplan, D., and Vunjak-Novakovic, G. Bone and cartilage tissue constructs grown using human bone marrow stromal cells, silk scaffolds and rotating bioreactors. Biomaterials **27,** 6138, 2006.
41. Zhou, Y.F., Sae-Lim, V., Chou, A.M., Hutmacher, D.W., and Lim, T.M. Does seeding density affect *in vitro* mineral nodules formation in novel composite scaffolds? J Biomed Mater Res A **78A,** 183, 2006.
42. Sikavitsas, V.I., Bancroft, G.N., and Mikos, A.G. Formation of three-dimensional cell/polymer constructs for bone tissue engineering in a spinner flask and a rotating wall vessel bioreactor. J Biomed Mater Res **62,** 136, 2002.
43. Xu, Y., Malladi, P., Chiou, M., Bekerman, E., Giaccia, A.J., and Longaker, M.T. *In vitro* expansion of adipose-derived adult stromal cells in hypoxia enhances early chondrogenesis. Tissue Eng **13,** 2981, 2007.
44. Malladi, P., Xu, Y., Chiou, M., Giaccia, A.J., and Longaker, M.T. Effect of reduced oxygen tension on chondrogenesis and osteogenesis in adipose-derived mesenchymal cells. Am J Physiol Cell Physiol **290,** C1139, 2006.
45. Muschler, G.F., Boehm, C., and Easley, K. Aspiration to obtain osteoblast progenitor cells from human bone marrow: the influence of aspiration volume. J Bone Joint Surg Am **79A,** 1699, 1997.
46. Peptan, I.A., Hong, L., and Mao, J.J. Comparison of osteogenic potentials of visceral and subcutaneous adipose-derived cells of rabbits. Plast Reconstr Surg **117,** 1462, 2006.
47. Holtorf, H.L., Jansen, J.A., and Mikos, A.G. Flow perfusion culture induces the osteoblastic differentiation of marrow stromal cell-scaffold constructs in the absence of dexamethasone. J Biomed Mater Res **72A,** 326, 2005.
48. Chojkier, M., Houglum, K., Solisherruzo, J., and Brenner, D.A. Stimulation of collagen gene expression by ascorbic acid in cultured human fibroblasts—a role for lipid peroxidation. J Biol Chem **264,** 16957, 1989.
49. Choi, K.M., Seo, Y.K., Yoon, H.H., Song, K.Y., Kwon, S.Y., Lee, H.S., and Park, J.K. Effect of ascorbic acid on bone marrow-derived mesenchymal stem cell proliferation and differentiation. J Biosci Bioeng **105,** 586, 2008.
50. Lin, T.M., Tsai, J.L., Lin, S.D., Lai, C.S., and Chang, C.C. Accelerated growth and prolonged lifespan of adipose tissue-derived human mesenchymal stem cells in a medium using reduced calcium and antioxidants. Stem Cells Dev **14,** 92, 2005.
51. Atmani, H., Chappard, D., and Basle, M.F. Proliferation and differentiation of osteoblasts and adipocytes in rat bone marrow stroma cell cultures: effects of dexamethasone and calcitriol. J Cell Biochem **89,** 364, 2003.

52. Schwartz, Z., Weesner, T., van Dijk, S., Cochran, D.L., Mellonig, J.T., Lohmann, C.H., Carnes, D.L., Goldstein, M., Dean, D.D., and Boyan, B.D. Ability of deproteinized cancellous bovine bone to induce new bone formation. J Periodontol **71,** 1258, 2000.
53. Mauney, J.R., Jaquiery, C., Volloch, V., Herberer, M., Martin, I., and Kaplan, D.L. *In vitro* and *in vivo* evaluation of differentially demineralized cancellous bone scaffolds combined with human bone marrow stromal cells for tissue engineering. Biomaterials **26,** 3173, 2005.
54. Gratzer, P.F., Harrison, R.D., and Woods, T. Matrix alteration and not residual sodium dodecyl sulfate cytotoxicity affects the cellular repopulation of a decellularized matrix. Tissue Eng **12,** 2975, 2006.
55. Cowles, E.A., DeRome, M.E., Pastizzo, G., Brailey, L.L., and Gronowicz, G.A. Mineralization and the expression of matrix proteins during *in vivo* bone development. Calcif Tissue Int **62,** 74, 1998.

Address correspondence to:
Gordana Vunjak-Novakovic, Ph.D.
Department of Biomedical Engineering
Columbia University
622 W 168th St., VC 12-234
New York, NY 10032

E-mail: gv2131@columbia.edu

Received: March 11, 2009
Accepted: August 12, 2009
Online Publication Date: September 16, 2009